Journal of Biomedical Optics 5(2), 229–236 (April 2000)

Optical imaging as an adjunct to sonograph in differentiating benign from malignant breast lesions

Quing Zhu
University of Connecticut
Department of Electrical and Computer Engineering
Storrs, Connecticut 06269

Emily Conant
University of Pennsylvania
Radiology Department
Philadelphia, Pennsylvania 19104

Britton Chance
University of Pennsylvania
Department of Biophysics and Biochemistry
Philadelphia, Pennsylvania 19104

Abstract. The role of near infrared (NIR) diffusive light imaging as an adjunct to ultrasound in differentiating benign from malignant lesions was evaluated in 27 mammography patients with infiltrating ductal carcinomas, apocrine metaplasia, fibroadenomas, radial scar and ductal hyperplasia, cysts, and normal tissues. Conventional ultrasound/mammography images were graded based on BI-RADS assessment categories. The spatial NIR measurements were made at wavelengths of 750 and 830 nm. Functional images, such as relative changes of deoxyhemoglobin (deoxyHb) and total blood concentration, were estimated from the dual wavelength measurements. Maximum relative deoxyHb and blood concentration changes were measured, and spatial correlation of masses in relative deoxyHb and blood concentration images for each breast were calculated. For the five biopsy proven benign lesions, ultrasound/mammography diagnoses were suspicious for malignancy (four cases) and highly suspicious for malignancy (one case). Four lesions showed less than 1.0 V maximum deoxyHb and less than 1.5 V maximum blood concentration levels on average and spatial image correlation showed no correlated masses in both deoxyHb and blood concentration images. For the four biopsy proven malignant lesions, ultrasound/mammography diagnoses were highly suspicious for malignancy. Maximum deoxyHb and blood concentration changes were greater than 2.9 V on average except one lesion which showed smaller deoxyHb signal (maximum 0.85 V) but the deoxyHb mass and blood concentration mass were highly correlated. [S1083-3668(00)00502-5]

Keywords: diffusive light imaging; ultrasound imaging; breast cancer detection; diagnosis.

Paper JBO-42018 received Sep. 28, 1999; revised manuscript received Feb. 22, 2000; accepted for publication Feb. 22, 2000.

1 Introduction

Ultrasound is frequently used in conjunction with mammography to differentiate simple cysts from solid lesions. When the criteria for a simple cyst are strictly adhered to, the accuracy of ultrasound is 96%–100%.[1] However, the sonography appearance of benign and malignant lesions has considerable overlapping features which has prompted many radiologists to recommend biopsies on most solid nodules.[2–11] This results in a large number of biopsies yielding benign breast masses or benign breast tissue (currently 70%–80% of biopsies yield benign changes[12]). Most recently sonography has been used to distinguish between benign and malignant solid masses.[13] Stavros, Thickman, and Rapp have evaluated the ability of ultrasound to distinguish benign from malignant solid breast lesions.[13] In his series, a total of 750 palpable solid breast lesions were studied. Despite the known overlap features in some lesions, ultrasound was able to correctly classify 123 of 125 malignant lesions as indeterminate or malignant.

In this paper, we introduce the use of optical imaging as an adjunct to ultrasound in differentiating benign from malignant lesions. We demonstrate that optical imaging may provide diagnostic information that may help further differentiate benign from malignant breast lesions, thereby improving ultrasound specificity and reducing unnecessary biopsies.

Recently, optical diagnostics, based on diffusing near infrared (NIR) light, have been employed in breast cancer detection.[14–20] Functional imaging with NIR light is made possible in a spectrum window that exists within tissues in the 700–900 nm NIR region, in which photon transport is dominated by scattering rather than absorption. To a very good approximation, NIR photons diffuse through relatively thick tissues, such as several centimeters of a human breast. Functional imaging with NIR light offers several novel tissue parameters that differentiate tumors from normal breast tissue. For example, hemoglobin desaturation in tumors may be increased due to the high oxygen demand of cancers,[20–22] and blood volume may be increased over that of normal background tissue due to the metabolic needs of cancers.[23,24]

While NIR imaging provides novel tissue parameters to improved tumor specificity, its relatively low resolution makes it unsuitable for morphological diagnosis. Its resolution is intrinsically limited by the diffusive nature of NIR light in

Address correspondence to Quing Zhu; electronic mail: zhu@engr.uconn.edu

1083-3668/2000/$15.00 © 2000 SPIE

tissue. Currently, typical instruments can distinguish simple structures of approximately 1 cm in size; sharp edges are typically blurred by a few millimeters.[25] By utilizing complementary features of ultrasound and NIR imaging, i.e., ultrasound gray scale imaging capability and optical tissue parameters, the combined diagnostic has a potential to overcome the deficiencies of either imaging technique.[26,27] This study reports the clinical evidence that low resolution NIR imaging can be used as an adjunct tool to conventional ultrasound following the mammography examination.

2 Materials and Methods

Between September 1997 and December 1997, 27 patients with suspicious mass determined by palpation and mammography were selected for this study. These patients were referred to the University of Pennsylvania Breast Imaging Section. All patients were scanned by ultrasound performed with a 7.5 MHz transducer on a commercial real-time gray scale scanner (Acoustic Imaging Technologies). After the routine sonographic examination was completed, the radiologist (E.C) supervised a research assistant (S.H) to position a NIR scanner over the ultrasonically detected mass and to start the NIR scan.

The ultrasound and mammography images were graded by the experienced radiologist (E.C) using the BI-RADS assessment categories of: (1) negative or normal, (2) benign changes, (3) probably benign, (4) suspicious: biopsy needed and, (5) highly suspicious for malignancy: biopsy needed. Among these 27 patients, 18 of them were classified as categories 1 and 2, four as category 4 and five as category 5. Biopsies were performed on all category 4 or 5 lesions.

The principle of NIR amplitude cancellation imaging has been detailed in Ref. 28 and the NIR imager used in this study was described in Ref. 20. Briefly, two wavelengths, namely 750 and 830 nm, have been employed by the imager. Since the deoxyHb absorption spectrum reaches its peak value around 750 nm and oxyHb and deoxyHb absorption spectrums have isosbestic wavelength at 830 nm, subtraction of the spatial measurements at these two wavelengths provides the best estimate of deoxy distribution of the medium. The blood concentration or volume is well approximated by the sum of the absorbances at the two wavelengths, appropriately weighted to minimize the response to oxygenation and deoxygenation changes. The imager based on amplitude cancellation appears to have good sensitivity to absorption changes. However, since each cancellation signal was obtained in hardware by subtraction of received signals from two equidistance detectors, quantitative calculation of absorption coefficients and therefore estimation of deoxyHb, oxyHb, and blood concentrations from the direct cancellation measurements was difficult. Since the objective of this study is to assess the potential role of optical imaging in aiding conventional breast imaging, sensitivity is the main concern. We have used relative amplitude changes in voltage scales in our image calculations.

The NIR probe consists of eight laser diode sources (four for each wavelength) and 21 silicon detectors (see Figure 1). The source and detectors were distributed in a $10 \times 10\,\mathrm{cm}^2$ rubber pad which could be compressed against the breast during examination. The sources were modulated at 2 kHz frequency. The four source pairs and 21 detectors were time shared in a multiplex system controlled by a PC. Each source and a pair of two equidistance detectors formed one cancellation signal and a total of 72 signals were formed from all possible source and two equidistance detector combinations. These 72 signals were interpolated four times and were back-projected to form an *x-y* spatial image at each wavelength. Subtraction of the images obtained at the two wavelengths provided an estimate of relative deoxy functional image and weighted sum provided an estimate of relative blood volume functional image.

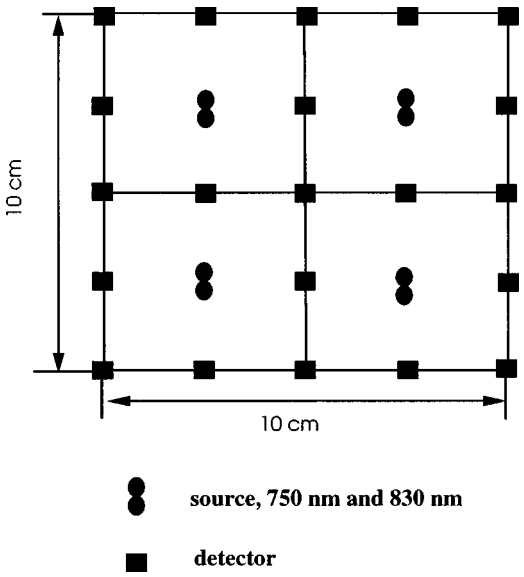

Fig. 1 Source and detector configuration of the 2D NIR probe.

The two-dimensional (2D) optical array provides a spatial *x-y* image of the examined breast while a commercial ultrasound probe provides *x-z B*-scan slices. The term *z* is the propagation direction toward the chest wall. It would be desirable to co-register both optical and acoustic images at the same views, so that the lesion shape, size, and depth can be compared directly. However, such co-registration requires 2D ultrasound arrays which can provide *x-y C*-scan images.[29] Since such arrays are not commercially available, we do not attempt to seek absolute co-registration in this preliminary study but we do use NIR parameters to provide additional diagnostic information to further classify ultrasound detected lesions.

Since malignant lesions are likely correlated with hypoxia[21,22] and angiogenesis,[23,24] a correlation of masses in both deoxyHb and blood concentration images can be used as a criterion to characterize the malignancy. In addition, this criterion is robust to any image artifacts that may appear in either deoxyHb or blood volume images. The spatial correlation measure used in this study is the normalized correlation between pixels[30] in a same spatial window of the deoxyHb and blood volume images

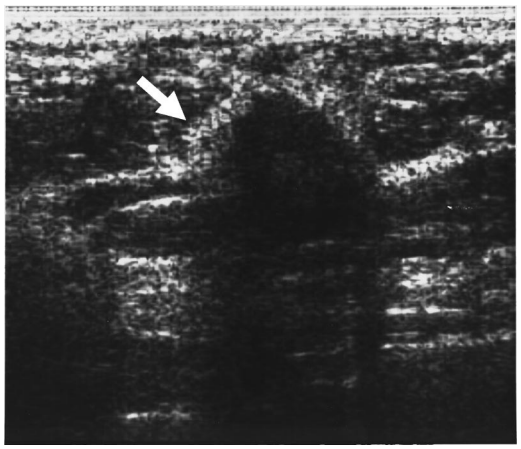

Fig. 2 An 85-year-old woman with a palpable lump. Sonogram shows an irregular poorly defined hypoechoic mass with characteristic malignant features, including angular margin, vertical growth pattern, and shadowing. Biopsy revealed that the lesion was infiltrating ductal carcinoma.

$$\rho_{(i,j)}=\left[\sum_p \sum_q \text{deoxy}_{(p,q)} BV_{(p,q)} \Big/ \left(\left(\sum_p \sum_q \text{deoxy}^2_{(p,q)}\right)^{1/2} \sum_p \sum_q BV^2_{(p,q)}\right)^{1/2}\right],$$

where $\text{deoxy}_{(p,q)}$ and $BV_{(p,q)}$ are the image pixel values of deoxyHb and blood volume images inside the window, and i and j are the coordinates of the center of the window. The window size used is 2.4 cm by 2.4 cm. The center of the window is moved pixel by pixel until all the correlation coefficients were calculated. A 0.995 threshold is used for the correlation image.

3 Results

Figure 2 shows a gray scale ultrasound image of a palpable lump in an 85-year-old woman. The horizontal and vertical axes correspond to lateral dimension and propagation depth, respectively. Skin surface is at the top of the image. The sonogram shows an irregular poorly defined hypoechoic mass with characteristic malignant features, including angular margin, vertical growth pattern, and shadowing. The mass center is located at approximately 1.5 cm depth. The diagnosis was highly suspicious for malignancy (category 5) and biopsy revealed that the lesion was infiltrating ductal carcinoma. Figure 3 shows the corresponding optical deoxyHb (a) and blood volume (b) images of the lesion. The horizontal and vertical axes correspond to x and y spatial positions of the probe shown in Figure 1. The images showed a significant amount of deoxyHb signal (maximum 2.1 V) and blood volume signal (maximum 2.6 V). The bars illustrated voltage levels of the gray scale coding and eight levels were used in the display. The spatial locations of the mass in both deoxyHb and blood volume images were correlated. Figure 3(c) showed the correlation map of deoxyHb and blood volume images and the correlation was high (greater than 0.995 threshold) at the lesion location.

As discussed earlier, the ultrasound view is in x-z (z is the propagation direction) and the optical view is in x-y spatial plane; direct comparison between ultrasound and optical images about the lesion shape and size cannot be obtained. Furthermore, since the ultrasound and optical probes are used separately to scan the deformable breasts, direct comparison between ultrasound and optical images about the spatial location of the lesion is difficult. However, optical images do provide diagnostic information that the lesion is hypoxia and has a significant amount of blood supply.

Figure 4 shows a gray scale scan of a palpable mass in a 27-year-old woman. The image reveals a 14 mm macrolobulated solid mass with irregular margins. The mass center is located at approximately 1.2 cm depth. These findings were suspicious (category 4), and ultrasound guided core biopsy was recommended. Biopsy yielded a benign fibroadenoma. Figure 5 shows deoxyHb (a) and blood volume (b) images. No discrete mass was found in the deoxyHb image and a diffused mass was found in the blood volume image (maximum 1.92 V). However, the correlation map indicated that the spatial distribution of the blood volume mass is not correlated with the corresponding deoxy area.

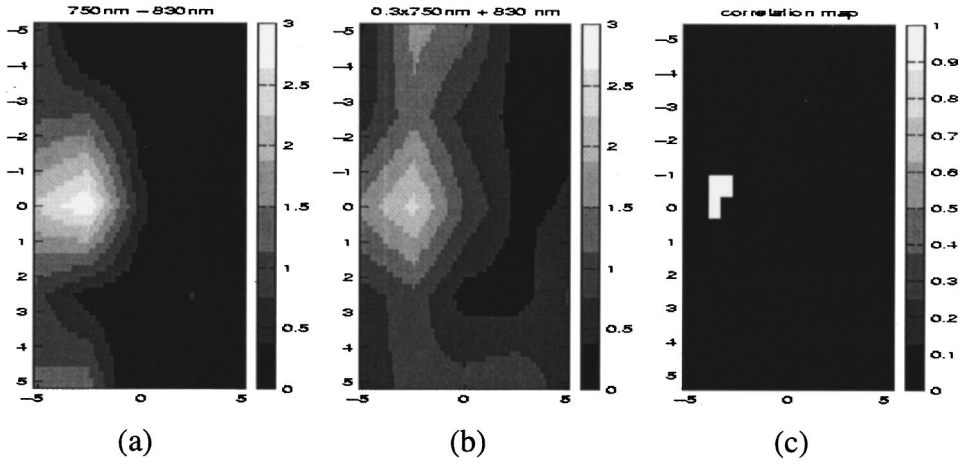

Fig. 3 Corresponding optical deoxyHb image (a), blood volume image (b), and mass correlation map (c) of the 85-year-old woman. Both deoxyHb and blood volume images showed significant changes and the masses were highly correlated.

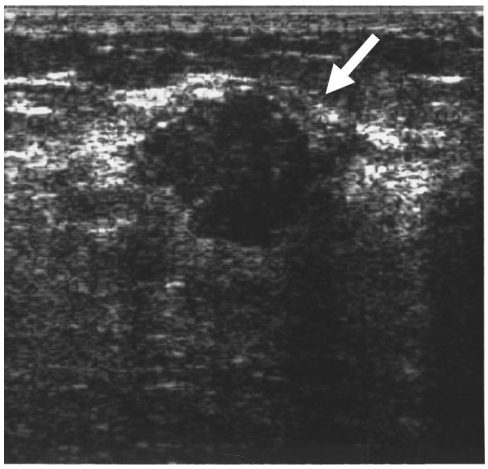

Fig. 4 Ultrasound image of a 27-year-old woman with a palpable left breast mass. The image reveals a macrolobulated mass with irregular margins. These findings are suspicious. Biopsy yielded a benign fibroadenoma.

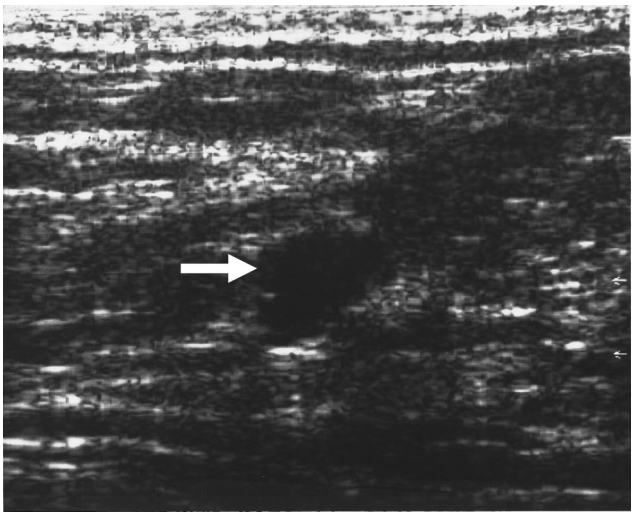

Fig. 6 A 59-year-old woman with a new 8 mm mass seen on screening mammography. Ultrasound revealed a hypoechoic indeterminate mass. The mass did not meet all the criteria for a simple cyst. Aspiration of the lesion was necessary to confirm that the lesion was a benign cyst.

Figure 6 shows a sonogram of a 8 mm mass in a 59-year-old woman. The mass center is located at approximately 1.8 cm depth. The new mass was seen on screening mammography. Ultrasound revealed a hypoechoic indeterminate mass that did not meet all the criteria for a simple cyst (category 4). Aspiration of the lesion was recommended to confirm that the lesion was a benign complex cyst. Corresponding optical images are shown in Figure 7. No discrete mass was found in the deoxyHb image (a) and a diffused mass was found in blood volume image (middle left) with a maximum value of 1.4 V. The correlation map revealed no correlated mass in both images.

Table 1 summarizes biopsy results (''gold'' standard), ultrasound/mammography, and optical findings of the total nine suspicious and highly suspicious lesions considered by ultrasound and mammography. The first cases represent biopsy proven benign lesions which included fibroadenoma, fibroadenoma and simple cysts, complex cyst, apocrine metaplasia and a radial scar, and ductal hyperplasia. The ultrasound/mammography diagnoses of the first four lesions were suspicious for biopsy (category 4) and the diagnosis of the last one was highly suspicious for malignant biopsy (category 5). These five patients underwent the necessary aspiration or biopsy to determine the nature of the lesion. The NIR images showed less than 1.0 V on average in deoxy images and less than 1.5 V on average in blood volume images except for the case of apocrine metaplasia. Image correlation of deoxyHb and blood volume masses showed no correlated masses in four benign lesions except the case of apocrine metaplasia.

The four malignant cases were infiltrating ductal carcinomas (IDC). The ultrasound/mammography diagnoses were highly suspicious for malignant biopsy (category 5). The NIR

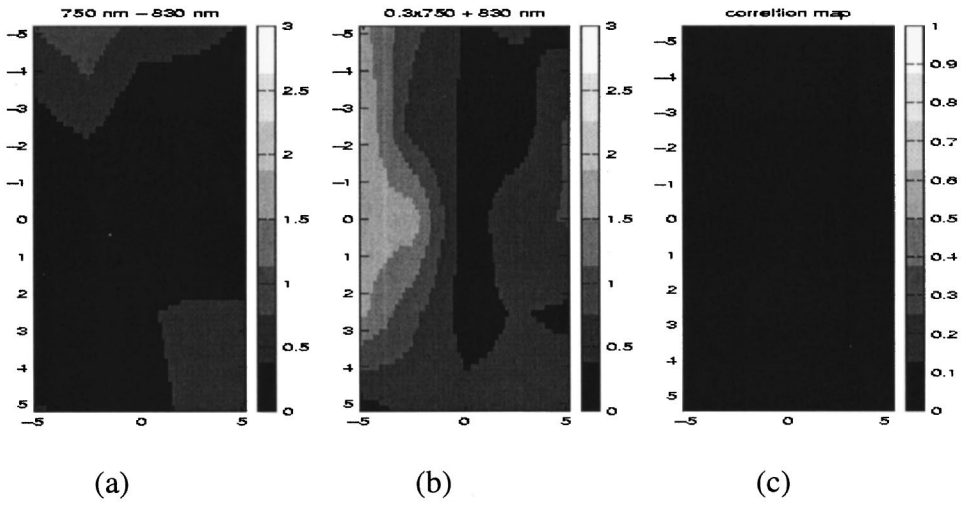

Fig. 5 Optical deoxyHb (a), blood volume (b), and similarity map (c) of the left breast of the 27-year-old woman. No significant changes in deoxyHb and blood volume images were found and no correlated masses in both images.

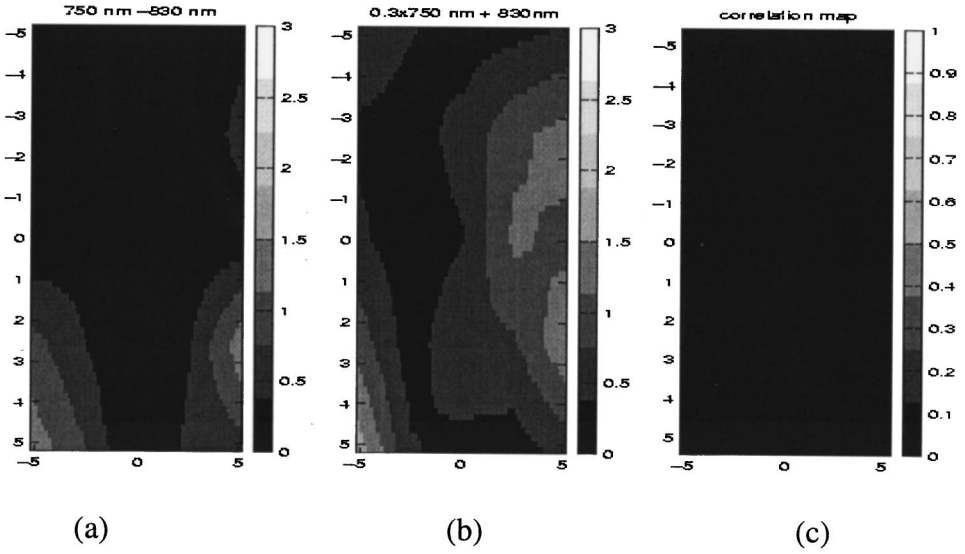

Fig. 7 Optical deoxyHb (a), blood volume (b), and similarity map (c) of the right breast of the 59-year-old woman. No significant changes in deoxyHb and blood volume images were found and no correlated masses in both images.

images showed greater than 2.9 V on average in deoxyHb and blood volume images in three cases. In one IDC case, the deoxy signal is small (peak 0.85 V) but the lesion location in deoxy and blood volume images is highly correlated.

The rest of the patients who had both ultrasound and mammography were considered to have normal breast tissue or simple cysts and biopsies were not recommended. Optical imaging was performed on these patients. The maximum deoxy level of this group on average is 1.37 V (±0.49 V) and the maximum blood volume level on average is 1.72 V (±0.61 V). These mean values are very close to the mean values of the four biopsy proven benign cases and are much lower than that of three biopsy proven malignant cases.

4 Discussion

Quantitative concentrations of deoxyHb, oxyHb, and blood can be estimated from the optical absorption coefficients measured at dual wavelength.[31,32] However, since the NIR imager used in these experiments provided different signals in hardware between all equidistance detectors, calculation of the absorption coefficients from the direct cancellation measurements was difficult. Therefore the deoxyHb and blood volume estimates were given in direct measurements using voltage scales and these estimates can be considered as relative changes of deoxyHb and blood volume.

Adjunctive techniques such as optical imaging are of potential clinical interest to improve specificity of conventional mammography and ultrasound imaging of the breast. Because the majority of breast biopsies yield benign tissue, there is considerable interest in techniques that could facilitate noninvasive differentiation of benign from malignant lesions. Optical imaging that provides functional parameters for differentiating benign from malignant lesions has the potential to improve specificity of breast cancer diagnosis and thus to reduce the number of biopsies that yield benign tissue.

We evaluated optical imaging as an adjunct tool to conventional ultrasound following the routine mammography in diagnosis of a variety of breast conditions. Estimated deoxyHb and blood volume functional parameters were jointly used to aid ultrasound/mammography in differentiating benign from malignant lesions. We have found that optical imaging has the potential to be valuable in differentiating lesions that are considered intermediate by conventional imaging. For five biopsy confirmed benign lesions, ultrasound/mammography diagnoses were indeterminate or suspicious enough to require biopsy. However, in four of the five lesions requiring biopsy based on conventional imaging, four lesions did not show significant deoxy and blood volume changes (maximum values less than 1.5 V) and the masses in deoxy and blood volume images did not show any correlation. These NIR findings were consistent with NIR changes found in normal and benign cases (categories 1 and 2). The fifth case was histologically benign (apocrine metaplasia), but the deoxy and blood volume levels were in the range considered suspicious and the masses in both images were highly correlated.

For the four biopsy confirmed malignant lesions, ultrasound/mammography diagnoses were highly suspicious for biopsy. Three lesions of the four cases showed considerably high deoxy and blood volume changes (maximum values greater than 2.9 V). The fourth case showed lower level of deoxy but higher level of blood volume. However, the masses in deoxy and blood volume images were highly correlated for all four malignant cases suggesting that the degree of correlation of these two measures may be an important predictor of malignancy. This must be further evaluated with more patients.

Literature data clearly indicate that the mean oxygen partial pressure (PO_2) values in human breast tumors *in situ* are distinctly lower than in a normal breast.[21,22,33] However, literature data also suggest that there is marked tumor-to-tumor variability in hypoxia[22] which may count for the low deoxy cancer case in our study. Vaupel et al.[22] obtained statistics of PO_2 measurements from 15 breast cancer patients (1068 readings) and 16 normal breasts (1099 readings) and found that

Table 1 Comparison of biopsy, US (with knowledge of mammography) and NIR findings.

Biopsy (case No.)	US+mammo	NIR		
Benign* (5 cases)	Reading	deoxyHb	BV	Image correlation (0.995)
Fibroadenoma (1)	Suspicious (4)	0.99 V	1.92 V	No correlated mass in deoxy and *BV*
Fibroadenoma and cyst (1)	Suspicious (4)	0.95 V	1.65 V	No correlated mass
Complex cyst (1)	Suspicious (4)	1.38 V	1.41 V	No correlated mass
Radial scar and ductal hyperplasia (1)	Highly suspicious for malignancy (5)	0.75 V	1.04 V	No correlated mass
		avg. 1.02±0.26 V	1.51±0.37 V	
Apocrine metaplasia (1)	Suspicious (4)	2.08 V	1.91 V	Yes, correlated mass
Malignant* (4 cases)				
Infiltrating ductal carcinomas (3)	Highly suspicious for malignancy (5)	2.92±0.47 V	3.46±0.45 V	Yes, correlated mass
Infiltrating ductal carcinomas (1)	Highly suspicious for malignancy (5)	0.85 V	2.08 V	Yes, correlated mass
		avg. 2.41±1.10 V	3.12±0.78 V	
* Biopsy proven				
Normal breast tissue and Cysts $^{+}$(18 cases)	Normal and benign changes (1&2)	1.37±0.49 V	1.72±0.61 V	No correlated mass except for nipple artifacts (see discussion)
$^{+}$Nonbiopsy proven				artifacts (see discussion)

the PO_2 histograms of tumors were usually shifted to lower O_2 tensions with a median of 30 mmHg, whereas in the normal tissues and in fibrocystic disease the PO_2 distributions were more or less Gaussian with a median of 65 mmHg.

The window size used to calculate the correlation map between deoxy and blood volume images affects the computed correlation coefficients and the selection of threshold value. Larger window is more robust to correlation artifacts. However, larger window size smoothes adjacent image pixels and produces a larger correlated area in the correlation map when the masses in deoxy and blood volume images are correlated. Because of the spatial smoothing, the computed correlation coefficients using a larger window are smaller than those using a smaller window. Based on these considerations, the window size used in this paper was about the average mass size and the threshold was selected based on the window size.

A technical consideration in optical imaging of the breast is the fact that brown and dark nipples absorb more light than the surrounding tissue and appear as absorbers (''nipple artifacts'') in both wavelength measurements. Nipple artifacts may be confused with abnormal absorbers related to carcinoma. Since the deoxy image is the substraction of measurements obtained at the two wavelengths, it is less affected by the nipple artifacts. We have found that the magnitude of nipple artifacts in deoxy image is much lower than that of carcinoma but the nipple mass in deoxy and blood volume images are correlated in some cases. Among the total 54 breasts examined, eight cases showed a high correlation between deoxy and blood volume images at nipple locations. However, the maximum deoxy level on average at nipple locations is 1.30 V (±0.56 V) and maximum blood volume level on average is 1.88 V (±0.57 V) for these eight cases. These values are significantly lower than those of the three

malignant cases. Since the nipple can be easily recognized in ultrasound images, nipple artifacts in NIR images should be easily distinguished from cancers. This requires that the ultrasound and optical images be co-registered (see discussion below).

All patients were examined with separate ultrasound and NIR scans. In the cases of single lesions, there were no ambiguities in mapping lesions in both ultrasound and optical images. However, in the cases of multiple lesions, we had difficulty in mapping lesions. Especially, when the lesions are located closer to each other. Among the nine patients with lesions categorized as 4 and 5 by conventional imaging, one patient had two malignant lesions in the same breast. Ultrasound detected the two lesions but NIR images showed only one lesion with high deoxy (greater than 3 V) and high blood volume (greater than 3 V) changes. The correlation map showed a large area of correlated mass in this case. This spatial mapping uncertainty can be overcome by co-registration of optical and ultrasound images and by developing higher resolution optical imaging algorithms. We have developed a prototype scanner with ultrasound and NIR imaging arrays simultaneously deployed on the same hand-held two-dimensional probe.[27] The probe can provide spatially co-registered ultrasound and optical image slices of a three-dimensional (3D) tissue volume. With the co-registered images, the lesion size, shape, and location can be compared directly.

In conclusion, preliminary results suggest that NIR diffusive light imaging may have a potential role in differentiating benign from malignant lesions detected by conventional imaging. Since our study includes only a small population of scheduled diagnostic patients, the sensitivity/specificity of NIR combined with conventional breast imaging cannot be judged. However, incorporation of NIR into breast imaging may in the future help to improve the diagnostic specificity and thus to reduce the number of unnecessary biopsies.

Acknowledgments

The authors thank Yu Chen for assistance with the NIR data format. Q.Z. acknowledges partial support from the Army Medical Research and Materiel Command (DAMD-17-94-J-4133) and the University of Connecticut Research Foundation. B.C. acknowledges partial support from NIH (CA 60182 and CA 72895).

References

1. E. A. Sickles, ''Detection and diagnosis of breast cancer with mammography,'' *Perspect. Radiology* **1**, 36–65 (1998).
2. E. A. Sickles, R. A. Filly, and P. W. Callen, ''Benign breast lesions: Ultrasound detection and diagnosis,'' *Radiology* **151**, 467–470 (1984).
3. E. A. Sickles, R. A. Filly, and P. W. Callen, ''Breast cancer detection with sonography and mammography,'' *AJR, Am. J. Roentgenol.* **140**, 843–845 (1983).
4. L. W. Bassett and C. Kimme-Smith, ''Breast sonography,'' *AJR, Am. J. Roentgenol.* **156**, 449–455 (1991).
5. L. W. Bassett, C. Kimme-Smith, L. K. Sutherland, R. H. Gold, D. Sarti, and W. King, ''Automated and hand-held breast ultrasound: Effect on patient management,'' *Radiology* **165**, 103–108 (1987).
6. C. Cole-Beuglet, R. Z. Soriano, and B. Kurtz et al., ''Ultrasound analysis of 104 primary breast carcinomas classified according to histopathologic type,'' *Radiology* **147**, 191–196 (1983).
7. C. Cole-Beuglet, R. Soreano, and M. Pasto, et al. ''Solid breast lesions: Can ultrasound differentiate benign and malignant?,'' in *Ultrasonic Examination of the Breast*, J. Jellins and T. Kobayahsi, Eds., pp. 45–55, Wiley, New York (1983).
8. D. B. Kopans, J. E. Meyer, and K. K. Lindfors, ''Whole-breast US imaging: Four-year follow-up,'' *Radiology* **157**, 505–507 (1985).
9. V. P. Jackson, ''The role of US in breast imaging,'' *Radiology* **177**, 305–311 (1990).
10. V. P. Jackson, ''Sonography of malignant breast disease,'' *Semin, Ultrasound CT MR* **10**, 119–131 (1989).
11. L. A. Venta, C. M. Dudiak, C. G. Salomon, M. E. Flisak, ''Sonographic evaluation of the breast,'' *RadioGraphics* **14**, 29–50 (1994).
12. F. M. Hall, J. M. Storella, and D. Z. Silverstone et al., ''Non-palpable breast lesions: Recommendations for biopsy based on suspicious carcinoma of mammography,'' *Radiology* **167**, 353–358 (1988).
13. T. A. Stavros, D. Thickman, and C. Rapp, ''Solid breast nodules: Use of sonography to distinguish between benign and malignant lesions,'' *Radiology* **196**, 123–134 (1995).
14. S. Nioka, Y. Yung, M. Schnall, S. Zhao, S. Orel, C. Xie, and B. Chance, ''Optical imaging of breast tumor by means of continuous waves,'' *Oxygen Transport to Tissue XVII*, Neoto Em, Ed., Plenum, New York (1992).
15. S. Fantini, M. A. Franceschini, G. Gaida, E. Gratton, H. Jess, W. M. Mantulin, K. T. Moesta, P. M. Schlag, and M. Kashke, ''Frequency-domain optical mammography: Edge effect corrections,'' *Med. Phys.* **23**, 1–9 (1996).
16. M. A. Franceschini, K. T. Moesta, S. Fantini, G. Gaida, E. Gratton, H. Jess, M. Seeber, P. M. Schlag, and M. Kashke, ''Frequency-domain techniques enhance optical mammography: Initial clinical results,'' *Proc. Natl. Acad. Sci. USA* **94**, 6468–6473 (1997).
17. J. B. Fishkin, O. Coquoz, E. R. Anderson, M. Brenner, and B. J. Tromberg, ''Frequency-domain photon migration measurements of normal and malignant tissue optical properties in human subject,'' *Appl. Opt.* **36**, 10–20 (1997).
18. T. L. Troy, D. L. Page, and E. M. Sevick-Muraca, ''Optical properties of normal and diseased breast tissues: Prognosis for optical mammography,'' *J. Biomed. Opt.* **1**(3), 342–35 (1996).
19. R. J. Grable, D. P. Rohler, and S. Kla, ''Optical tomography breast imaging,'' *Proc. SPIE* **2979**, 197–210 (1997).
20. S. Zhou, Y. Chen, Q. Nioka, X. Li, L. Pfaff, C. M. Cowan, and B. Chance, ''A portable dual wavelength amplitude cancellation image system for the determination of human breast tumor,'' *Proc. SPIE* **3597**, 571–579 (1999).
21. P. Vaupel, ''Oxygen transport in tumors,'' in *Oxygen Transport to Tissue XVII*, Ince et al., Eds., Plenum, New York (1996).
22. P. Vaupel, K. Schlenger, C. Knoop, and M. Hockel, ''Oxygenation of human tumors: Evaluation of tissue oxygen distribution in breast cancers by computerized O_2 tension measurements,'' *Cancer Res.* **51**, 3316–3322 (1991).
23. J. Folkman, ''What is the evidence that tumors are angiogenesis dependent,'' *J. Natl. Cancer Inst.* **82**(1), 4–6 (1990).
24. J. Folkman and M. Kiagsbrun, ''Angiogenic factors,'' *Science* **235**, 442–446 (1987).
25. A. Yodh and B. Chance, ''Spectroscopy and imaging with diffusing light,'' *Phys. Today* **48**(3), 34–40 (1995).
26. Q. Zhu, D. Sullivan, B. Chance, and T. Dambro, ''Combined ultrasound and near infrared diffusive light imaging,'' *IEEE Trans. Ultrason. Ferroelectr. Freq. Control* **46**(3), 665–678 (1999).
27. Q. Zhu, T. Dunrana, M. Holboke, V. Ntziachristos, and A. Yodh, ''Imager that combines near infrared diffusive light and ultrasound,'' *Opt. Lett.* **24(15)**, 1050–1052 (1999).
28. B. Chance, K. Kang, L. He, J. Weng, and E. Sevick, ''Highly sensitive object location in tissue models with linear in-phase and anti-phase multi-element optical arrays in one and two dimensions,'' *Proc. Natl. Acad. Sci. USA* **90**, 3423–3427 (1993).
29. ''Section of ultrasonic transducers and arrays,'' *Ultrason. Symp. Proc.* **2**, 985–1098 (1998).
30. B. Steinberg, D. Sullivan, and D. Carlson, ''Disparity mapping applied to sonography of the breast: Technical note,'' *Radiology* **207**, 545–550 (1998).

31. E. M. Sevick, B. Chance, J. Leigh, S. Nioka, and M. Maris, ''Quantitation of time-and frequency-resolved optical spectra for the determination of tissue oxygenation,'' *Anal. Biochem.* **195**, 330–351 (1991).
32. T. McBride, B. W. Pogue, E. D. Gerety, S. B. Poplack, U. Osterberg, and K. Paulsen, ''Spectroscopic diffuse optical tomography for the quantitative assessment of hemoglobin concentration and oxygen saturation in breast tissue,'' *Appl. Opt.* **38**(25), 5480–5490 (1999).
33. P. Vaupel, F. Kallinowski, and P. Okunieff, ''Blood flow, oxygen and nutrient supply, and metabolic microenvironment of human tumors: A review.'' *Cancer Res.* **49**, 6449–6465 (1989).